ACADEMIC PRESS

Available online at www.sciencedirect.com
SCIENCE DIRECT®

Journal of Catalysis 218 (2003) 419–426

JOURNAL OF CATALYSIS

www.elsevier.com/locate/jcat

Extrusion of Cu/ZnO catalysts for the single-stage gas-phase processing of dimethyl maleate to tetrahydrofuran

Steffen Peter Müller, Martin Kucher, Christoph Ohlinger, and Bettina Kraushaar-Czarnetzki *

Institute of Chemical Process Engineering CVT, University of Karlsruhe, Kaiserstrasse 12, D-76128 Karlsruhe, Germany

Received 13 January 2003; revised 6 March 2003; accepted 10 March 2003

Abstract

Bifunctional catalysts consisting of copper, zinc oxide, and γ-alumina have been produced by means of extrusion. The effects of formulation and forming conditions on morphology, pore texture, and copper surface area are discussed. These extruded catalysts have been employed in the fixed-bed gas-phase conversion of dimethyl maleate at temperatures between 453 and 493 K and space velocities ranging from 0.2 to 2.4 h^{-1}. Copper catalyzes the hydrogenation and hydrogenolysis reactions yielding γ-butyrolactone, and 1,4-butanediol. γ-Alumina provides weakly acidic sites which promote the subsequent dehydration of 1,4-butanediol to tetrahydrofuran. Coupled products are methanol and water. Through choice of composition and pore texture of the extrudates it is possible to achieve tetrahydrofuran yields of 100% (basis the C_4-products) at a low pressure (2.5 MPa) in a single stage.

Keywords: Catalyst forming; Extrusion; Pore-size distribution; Maleic acid; Hydrogenation; Hydrogenolysis; Copper catalyst; Tetrahydrofuran

1. Introduction

Tetrahydrofuran (THF) is an important solvent for many polymers, and it is used as a monomer in the manufacture of polytetramethylene ether glycol (PTMEG), a precursor for polyurethanes, elastic fibers, molded elastomers, and copolyesters [1]. In view of the strongly growing markets for PTMEG, a doubling of the production of THF in the period between 1995 and 2004 has been forecasted [2].

THF is obtained through the dehydration of 1,4-butanediol (BDO) in the presence of mineralic acid or acidic ion exchangers. The major part of the BDO, in turn, is still produced via the Reppe process [3] using acetylene and formaldehyde as the feedstocks. New manufacturing routes, however, will be based on economically more attractive raw materials. Among these, maleic acid anhydride, which is available from the direct catalytic oxidation of *n*-butane or other linear C_4-hydrocarbons with air, will play a dominant role [4].

As shown in the reaction scheme in Fig. 1, the formation of BDO is possible both from maleic acid anhydride and from the corresponding dialkyl esters, e.g., dimethyl maleate. The subsequent hydrogenation or hydrogenolysis steps, respectively, are catalyzed by heterogeneous noble metal, nickel, or copper catalysts. Most existing processes are carried out in three-phase slurry reactors at pressures between 5 and 30 MPa and temperatures between 420 and 570 K, and the preferred feedstock is the anhydride [5]. In contrast, a gas-phase process is feasible only with the dialkyl esters of maleic acid as a feed because the boiling points of the anhydrides, in particular of the intermediate succinic anhydride, are too high in the pressure range of interest. Despite the requirement of an additional esterification step upflow, a gas-phase process for the production of BDO would be very attractive because established fixed-bed reactor technology can be utilized, and lower pressures (between 2 and 7 MPa) can be applied. So far, only one gas-phase process has been established by Davy McKee Ltd. [6] which consists of two stages. A potential problem in gas-phase operation comprises fouling and plugging of the fixed-bed by polymeric material [7,8]. The polymeric deposits (polyesters) can be formed upon *trans*-esterification of dialkyl esters of maleic or succinic acid with the product BDO.

We recently investigated the conditions at which fouling and plugging by the viscous by-products occur. Our results indicate that the polyester formation is initiated by capillary

* Corresponding author.
E-mail address: bettina.kraushaar@ciw.uni-karlsruhe.de (B. Kraushaar-Czarnetzki).

0021-9517/03/$ – see front matter
doi:10.1016/S0021-9517(03)00157-X

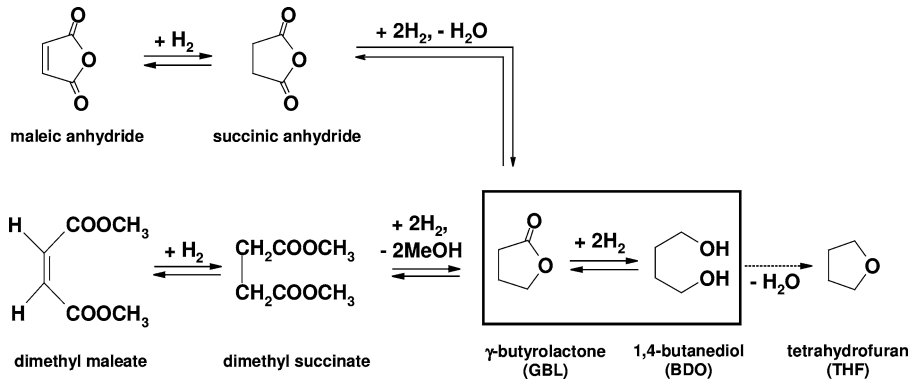

Fig. 1. Scheme of the hydrogenation and hydrogenolysis reactions of maleic acid derivatives to GBL and BDO, and of the subsequent dehydration to THF.

condensation of reactants, in particular of BDO, in the pores of the catalyst. Condensation can be prevented by applying high molar feed ratios of hydrogen to dimethyl maleate, i.e., by dilution of the organic reactants. We calculated the minimum H_2/maleate feed ratios required for safe and stable processing in a wide range of reaction pressures and temperatures and validated these calculated limits by processing experiments [9]. Hence, the single-stage gas-phase hydrogenation of dimethyl maleate in a fixed-bed reactor is a feasible option. Depending on the pore-size distribution of the catalyst, however, the required dilution with hydrogen may be extremely high.

Here, we report on novel extruded catalysts with bifunctional properties which provide a solution to this problem. In addition to the hydrogenating function, the catalysts comprise weakly acid sites which catalyze selectively the dehydration of BDO to THF. Because BDO is consumed, together with dimethyl succinate being the most critical compound with respect to capillary condensation, and because THF exhibits considerably lower Antoine constants than the other C_4-reactants [9], it will be possible to apply much lower H_2/maleate feed ratios without running into the regime of fouling by polymer formation. The other interesting aspect of this catalyst represents the possibility of producing THF from dimethyl maleate in a single rather than two stages, thereby using the most convenient, i.e., fixed-bed, reactor technology.

The catalysts used in our study contain copper and zinc oxide (Cu/ZnO). The active sites for hydrogenation and hydrogenolysis reactions are provided by metallic copper. The role of ZnO as an adsorbent for succinic anhydride has been elucidated recently by Herrmann and Emig who investigated the hydrogenation of maleic acid anhydride in the liquid (slurry) phase [10,11]. The gas-phase conversion of dimethyl maleate has been studied by Turek and coworkers [8,12]. These authors found that the hydrogenolysis of dimethyl succinate rather than the hydrogenation of the double bond in dimethyl maleate is the rate-limiting step. The corresponding rate coefficient can be related directly to the copper surface area [12]. At conversions of dimethyl succinate above ca. 80%, the temperature- and pressure-dependent thermodynamic equilibrium in the hydrogenation of γ-butyrolactone (GBL) to BDO is attained over Cu/ZnO catalysts [8,9]. The subsequent dehydration of BDO to THF plays a minor role because Cu/ZnO does not exhibit sufficient acidity.

In the catalysts reported here, the acid sites are provided by γ-Al_2O_3 which, in addition, acts as mechanically strong and porous binder for the embedded Cu/ZnO particles. Industrial Cu/ZnO catalysts [13–15] as well as those described in the literature are formed by pelleting. In contrast, our catalysts are formed by extrusion. Because the extent of compression and compaction is much lower in extrusion, the resulting catalysts exhibit larger pores and a higher porosity, and they allow for a higher effectiveness factors in the conversion of dimethyl maleate when used in the sizes convenient for a technical fixed-bed reactor. To our knowledge, this is the first report on the forming and application of Cu/ZnO extrudates.

2. Experimental

2.1. Catalyst preparation

The carbonate precursor of the catalyst was prepared by dropwise mixing of 1 M aqueous Na_2CO_3 (Merck, purity $>$ 99.9% m/m) solution with an aqueous solution containing 0.5 M, each, copper and zinc nitrate (Merck, $Cu(NO_3)_2 \cdot 3H_2O$, $>$ 99.5% m/m and $Zn(NO_3)_2 \cdot 6H_2O$, $>$ 99.0% m/m) under vigorous stirring at 359 K and a constant pH of 7. After cooling down, the precipitate was filtrated, washed several times with deionized water, and dried at 353 K for 16 h.

To produce a paste for extrusion, the dried copper/zinc carbonate precursor was mixed with boehmite (Sasol, impurities: $Fe_2O_3 < 200$ ppm, $Na_2O < 50$ ppm, $SiO_2 < 250$ ppm) and 22% m/m water in a rheo-kneader (Polydrive, Haake) at a constant temperature of 293 K and a rotor speed of 40 min^{-1}. Upon heating above 723 K, boehmite (AlO(OH)) undergoes a phase transition to γ-Al_2O_3. The proportions of metal carbonates and boehmite were chosen such that the percentage (c) of copper/zinc carbonate pre-

cursor in the water-free extrudate according to

$$c = 100 \cdot \frac{(m_{CuCO_3} + m_{ZnCO_3})}{(m_{CuCO_3} + m_{ZnCO_3} + m_{\gamma\text{-}Al_2O_3})}\% \quad (1)$$

amounted to 25, 50, and 75% m/m, respectively. Note that symbols are explained at the end of this article. The paste was transferred to a piston extruder and formed to cylindrical greenbodies (designation for ceramic bodies prior to heat treatment) with a diameter of 2 mm and a length of about 400 mm. The greenbodies were dried at room temperature and cut into pieces of about 5 mm length. The particles were transferred to a rotary kiln, heated at a rate of 2 K/min, and calcined in air for 3 h at 823 K. At this stage, the metal carbonates are transformed into the oxides, and the binder particles build a strong matrix of γ-alumina.

2.2. Characterization

The morphology of particles of the zinc/copper carbonate precursor was examined by means of scanning electron microscopy (Hitachi S-4500). The particle-size distribution of these precursor particles in aqueous suspension containing 1 g/L of solid was measured by means of laser diffraction (H9236, Sympatec Helos). Mercury intrusion (Autopore III, Micromeritics) was used to characterize porosities and pore-size distributions of the finished extrudates. Prior to the measurements, the extrudates were dried for 2 h at 393 K. The specific copper surface areas were measured by means of nitrous oxide (N_2O) decomposition at atmospheric pressure after reducing the CuO in the extrudates with hydrogen (purity: 99.999% m/m). The reduction was carried out with 3% H_2 in helium (purity: 99.996% m/m) at a volumetric flow rate of 300 cm^3/min (STP). After raising the temperature from 413 to 513 K at a rate of 20 K/h, the diluted hydrogen stream was replaced stepwise by pure hydrogen within 1 h. Finally, the samples were cooled to 333 K in pure helium and exposed to a flow of 100 cm^3/min (STP) of 0.1% N_2O in helium. The copper surface areas were calculated from the consumed amount of nitrous oxide according to the method described by Chinchen et al. [16].

2.3. Catalytic experiments

The catalytic experiments were carried out in a continuous flow unit equipped with a stainless-steel fixed-bed tubular reactor and on-line gas analysis. The catalyst bed had a diameter of 13 mm and a length of approximately 40 mm and consisted of extrudates diluted with nonreactive silicon carbide particles exhibiting a mean diameter of 0.5 mm in a mass ratio of 2:1. Upflow, the reactor void volume was filled with pure SiC particles in order to ensure a plug flow profile of the feed when contacting the catalyst bed. Prior to the experiments, the catalysts were reduced in situ at atmospheric pressure in the same way as described above for the measurement of the copper surface. Hydrogen and evaporated dimethyl maleate (purity: > 95% m/m) were fed into the reactor at a molar ratio of 250, a total pressure of 2.5 MPa, and hydrogen flow rates varying from 150 to 1000 cm^3/min (STP). The resulting residence times (t_{mod}) ranged between 0.8 and 13.5 s g/cm^3, which is equivalent to space velocities (WHSV) between 0.2 and 2.4 h^{-1}. The reaction temperatures ranged from 453 to 513 K. On-line analysis was carried out on a Hewlett Packard 5890 II gas chromatograph equipped with a CP-Wax 52 CB column after pressure release and addition of nitrogen (purity: 99.996% m/m) as an internal standard. The mean deviation in the product selectivities reported ranges from ±8% for low conversion levels to ±4% for full conversion.

3. Results and discussion

3.1. Morphology of the extrudates

Extrusion experiments were carried out with both the carbonate precursor of Cu and Zn and the oxides obtained after calcination. In any case, the extrusion of the pastes was difficult. Many trials were necessary to identify the compositions suitable to obtain stable and smooth extrudates, and these compositions are reported in the experimental part. Eventually, the carbonate precursor was preferred as a raw material because one additional calcination step can be avoided in this way. A decisive factor for the quality of extrudates is the rheological behavior of the paste. In the case of Cu/Zn-containing material, very small variations in the water content (±1% m/m) result in dramatic changes in the rheological properties. A low proportion of water results in a highly viscous, brittle paste with low plasticity which cannot be pressed through the nozzle of the extruder. When the amount of water is too high, the greenbodies become fissured and scaly as soon as they leave the nozzle (Fig. 2a). Most beneficial for extrusion is a plastic paste which does not display viscous flow in the nozzle but rather undergoes deformation, thereby forming a thin liquid film at the wall which enables slipping (wall slip behavior). As shown in

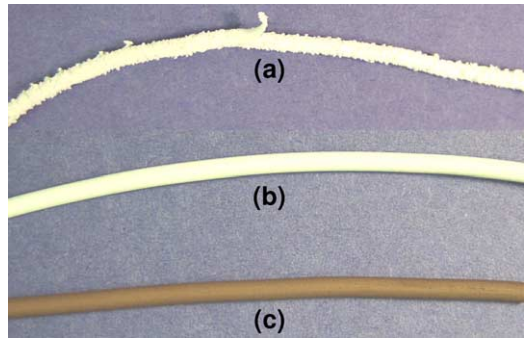

Fig. 2. Extruded strings produced from pastes containing boehmite, Cu- and Zn-carbonate. (a) Greenbody with surface defects, water content of the paste > 22% m/m. (b) Smooth greenbody, water content of the paste = 22% m/m. (c) Extruded string after calcination.

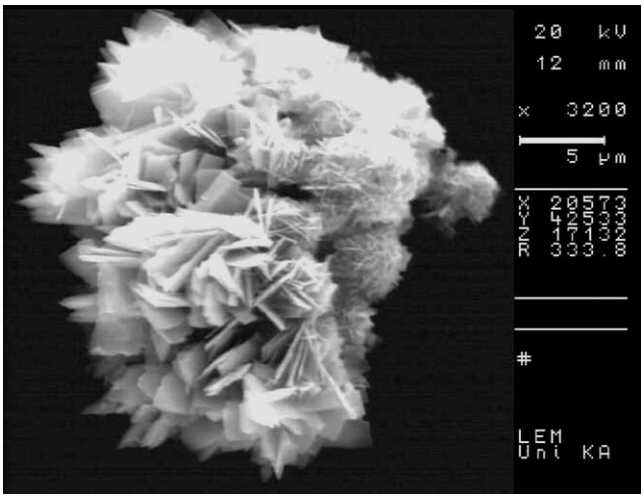

Fig. 3. SEM micrograph of Cu/Zn-carbonate crystals (Cu:Zn = 1:1).

Fig. 2b, the resulting greenbodies are straight and exhibit a smooth surface. Upon subsequent calcination, the color changes from light greenish blue to brown because of the transformation of $CuCO_3$ into CuO (Fig. 2c).

3.2. Pore texture and strength

Extrudates can be conceived as formed agglomerates of small particles. During calcination, at least a part of the particles representing the framework will form interconnecting solid bridges, be it by condensation reactions or by a certain degree of sintering. The voids in-between the particles represent the pores. Hence, porosity and pore-size distribution of extrudates depend on the size distribution of the particles representing the framework.

The boehmite particles used as a binder are of spherical shape and exhibit a mean diameter of 45 nm. In contrast, the particles of the Cu/Zn carbonate precursor are very large. As shown in Fig. 3, the particles are large intergrowths of fragile, plate-like crystals. Accordingly, the particle volume-size distribution q_3 (i.e., the derivative of the cumulative volumetric size distribution as a function of the equivalent diameter) of the material is characterized by a bimodal population (Fig. 4). The major part of the particles exhibits a mean diameter of 16.4 µm. The second peak in the size distribution resulting from particles of 2–3 µm is probably originating from fragments of the intergrowths.

When extrudates are formed from such a material together with binder particles of much smaller size, a pore-size distribution with three size maxima can be expected. This is shown in Fig. 5 for three calcined extrudates of equal composition ($c = 75\%$ m/m). The smallest pores (6 nm) predominantly represent the voids between the binder particles. The two types of macropores stem from voids between Cu/Zn oxide particles. The difference between the samples refers to the duration of kneading prior to extrusion. With increasing kneading time, i.e., mechanical energy input, a larger portion of the intergrowths of the carbonate precursor is broken

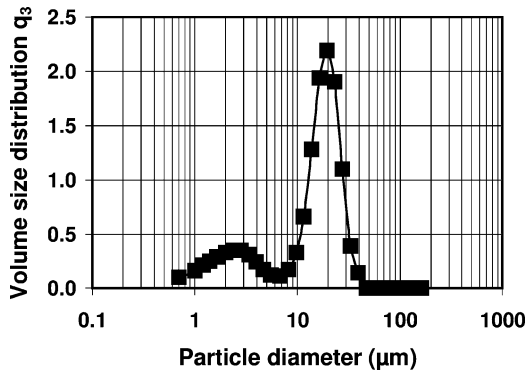

Fig. 4. Particle volume-size distribution q_3 of the Cu/Zn-carbonate crystals.

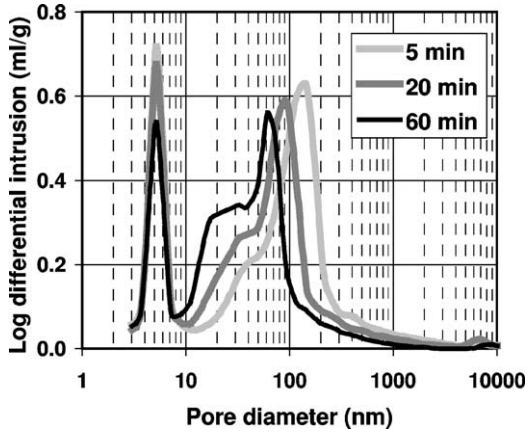

Fig. 5. Effect of the kneading time of the extrusion paste on the pore-size distribution of the resulting, calcined extrudates with $c = 75\%$ m/m.

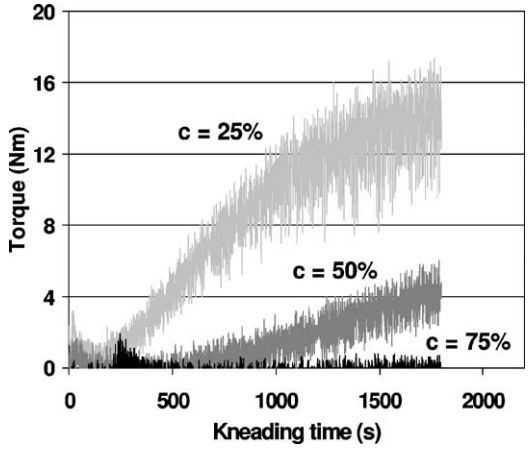

Fig. 6. Torque at the rotors of the kneader at a constant rotor speed of 40 min^{-1} as a function of the kneading time for three paste compositions (equal masses).

to smaller particles and fragments. As a result, the size of the macropores in the extrudates shifts to lower values with increasing kneading time.

Obviously, the pore-size distribution in the extrudates must also depend on the solid composition because the respective particle sizes differ so much. In Fig. 6, three kneading diagrams are depicted which were produced with equal

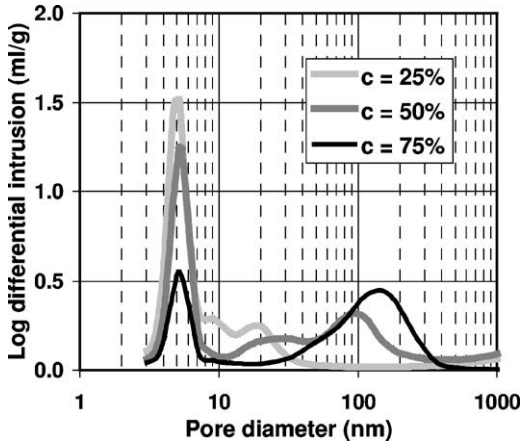

Fig. 7. Effect of the paste composition on the pore-size distribution of the resulting, calcined extrudates after equal kneading times of 10 min. Light gray line: sample 25/10, dark gray line: sample 50/10, and black line: sample 75/10 (see Table 1 for the designation).

masses of pastes containing equal amounts of water, but differing in the concentration (c) of Cu/Zn carbonate. This diagram is useful because the input of mechanical energy is represented by the area below the curves, i.e., the time integral of the torque at the rotors of the mixer at constant rotor speed. It indicates that pastes containing a high amount of binder are exposed to higher shear forces than pastes with less binder and a higher value of c when mixed at the same rotor speed. The corresponding mercury intrusion plots of the calcined extrudates (kneading time 10 min in all cases) are shown in Fig. 7. Large macropores are present only if the solid content of Cu/Zn carbonate in the paste amounts to 50% or higher. Again, it can be seen that the size of the macropores shifts to lower values with increasing energy input. In contrast, mesopores dominate when the amount of binder is high, both because the small binder particles are prevailing and because the high shear forces result in a more pronounced breakdown of the Cu/Zn carbonate particles.

Porosities of a selection of finished extrudates are summarized in Table 1. In accordance with the previous discussion it can be stated that the porosity decreases with increasing proportion of small particles in the framework of the extrudate which are either added as such or which are produced by input of energy upon kneading.

A qualitative inspection of the mechanical properties by manual breaking or squeezing of the extrudates revealed that their strength increases with increasing amount of γ-alumina. In addition, the kneading time has a pronounced effect. For instance, sample 50/60 obtained with a kneading time of 60 min exhibits a bulk crush strength (according to the American standard ASTM D 4179) of 79.6 N, indicating excellent suitability for application in a large-scale fixed-bed reactor. In contrast, the same paste composition after 5 min kneading time yields extrudates with an insufficient bulk crush strength of 7.1 N. These few data can only give a flavor of the strong impact of formulation and forming

Table 1
Effect of paste composition and kneading time on the porosity of finished (calcined) extrudates

Sample designation	c (% m/m)	Kneading time (min)	Porosity (% v/v)
25/2	25	2	71.7
25/10	25	10	64.0
25/20	25	20	60.6
50/10	50	10	67.0
50/20	50	20	66.2
50/60	50	60	63.8
75/5	75	5	71.7
75/10	75	10	71.3
75/60	75	60	68.8

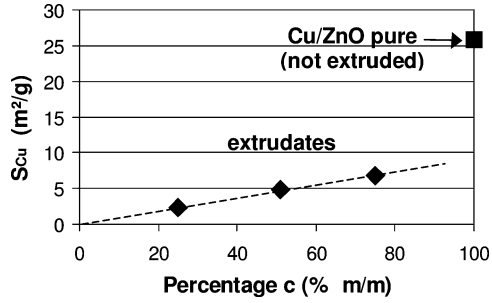

Fig. 8. Copper surface area of the extrudates as a function of the Cu/Zn content.

conditions on the applicability of catalysts in industrial-size reactors. We will devote more research to this issue in the near future.

3.3. Copper surface and activity

As shown in Fig. 8, the copper surface area of the extruded catalysts linearly increases with increasing copper content. In the same graph, we have also added the copper surface area of pure, nonextruded Cu/ZnO. This comparison indicates that the magnitude of the copper surface area is negatively affected by the catalyst formulation and forming. On the basis of earlier results reported by Schlander and Turek [8], one should expect that the activity of the catalysts in the conversion of dimethyl maleate follows the same trend as the copper surface area. The following proportionality should hold for equal modified residence time and equal temperature:

$$-\ln(1-X) \propto S_{\mathrm{Cu}}. \tag{2}$$

However, as shown in Fig. 9, our results indicate that the extruded catalysts are much more active than would be expected from the low values of their copper surface areas, this discrepancy being most pronounced at temperatures of 473 K or higher. It is important to note that the data of pure Cu/ZnO stem from tiny particles, (crushed pellets) with diameters ranging from 200 to 315 µm. Here, a negative effect of diffusional limitations can be excluded. The extrudates, in contrast, were all used in full size, i.e., with lengths of

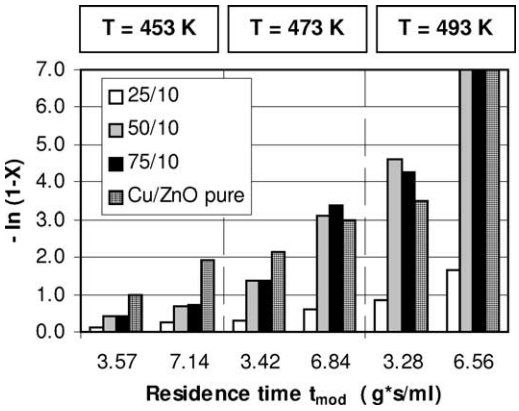

Fig. 9. Conversion of dimethyl succinate ($X_{\text{maleate}} = 100\%$ in all cases) as a function of the residence time for three reaction temperatures. Full-size extrudates of sample 25/10, white bars; sample 50/10, gray bars; and sample 75/10, black bars. Pure Cu/ZnO particles of diameter 200 to 315 μm, squared bars.

5 mm and diameters of 2 mm. It is the presence of γ-alumina which results in an enhancement of the DMS conversion. This effect is not to be ascribed to a hydrogenating function of this binder, but presumably to the fact that the hydrogenation products GBL and BDO are rapidly withdrawn from the respective equilibria because γ-alumina boosts the rate of the subsequent dehydration.

Also within the series of full-size extruded catalysts, there is no linear correlation between the activity (here expressed as $-\ln(1 - X)$) and the copper surface area. Fig. 9 shows that the extrudates with the highest copper surface area (sample 75/10, $c = 75\%$ m/m) display almost the same activity as those exhibiting medium copper surface area (sample 50/10 with $c = 50\%$ m/m). Tests carried out with extrudates of equal composition and different pore texture indicated that the reaction rates are limited by pore diffusion when the proportion of macropores is low. These preliminary results show that the apparent kinetics are influenced by the pore texture, and that the intrinsic activities of the extrudates are a function of both the copper surface area and the proportion of γ-alumina. A detailed kinetic analysis will be required, first in the absence of transport limitations (crushed extrudates), and subsequently using extrudates exhibiting different sizes and pore textures, to characterize quantitatively the effect of mass transport in extrudates. We will report on this work in the future.

3.4. Catalyst selectivity

The C_4-products formed over our catalysts are GBL, BDO, and THF. Fouling by polyester deposition was not observed. Other unwanted by-products such as 1-butanol or carbon dioxide were formed in negligible traces only, and the carbon mass balance was validated ($100 \pm 2\%$) in the experiments reported here. Hence, it is possible to define the integral (reactor) selectivity on the basis of molar fractions

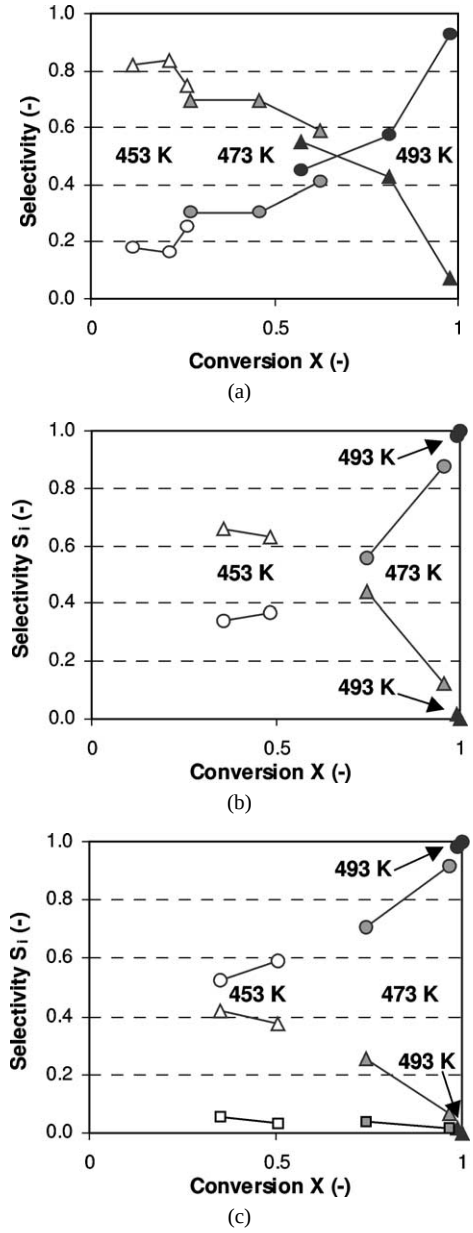

Fig. 10. Selectivity to C_4-products versus dimethyl succinate conversion at 453, 473, and 493 K and $p = 2.5$ MPa. Circles, THF; triangles, GBL; and squares, BDO. (a) Catalyst sample 25/10, (b) sample 50/10, and (c) sample 75/10.

of the C_4-products according to

$$S_i = \frac{x_{i,C_4}}{\sum x_{i,C_4}} \tag{3}$$

without taking the coupled production of methanol and water into account. In Fig. 10, the integral selectivities to C_4-products obtained at three different temperatures are depicted. The experiments were carried out with the catalyst samples 25/10, 50/10, and 75/10 (see Table 1 for the designation). In all cases, the THF selectivity increases with increasing conversion (i.e., increasing residence time) and temperature. Because THF is produced in the acid-catalyzed dehydration of BDO, the amount of weakly acidic

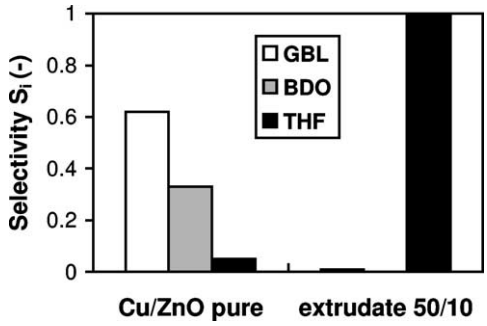

Fig. 11. Selectivity to C_4-products at a dimethyl succinate conversion of 98%. $T = 493$ K, $p = 2.5$ MPa.

γ-Al_2O_3 in the catalyst also has an effect. As can be seen in Fig. 10c, BDO is released only when the catalyst contains a low amount of γ-Al_2O_3 (sample 75/10). Higher concentrations of γ-Al_2O_3 result in a complete consumption of BDO.

To illustrate more clearly the effect of the acidic binder, a comparison is made in Fig. 11 between a catalyst consisting of pure Cu/ZnO and the alumina-bound extrudates 50/10. The selectivities to C_4-products are plotted for the same conversion of $X = 98\%$ at 493 K. The molar ratio BDO:GBL produced over pure Cu/ZnO approximately equals the thermodynamic equilibrium value at this temperature and pressure. Because of the relatively high temperature, a small amount of THF is formed as well. However, the dehydration does not disturb the equilibrium between GBL and BDO. In contrast, this equilibrium is completely shifted toward BDO because its subsequent dehydration is strongly accelerated when the alumina-bound catalyst is applied. This result is of technical importance because it means that the formation of THF is not thermodynamically limited by the pressure-dependent equilibrium reaction of GBL to BDO. Hence, very low reaction pressures can be applied in a single-stage process.

4. Conclusions

We have demonstrated that it is possible to produce THF yields of 100% from dimethyl maleate in a single stage by using a fixed-bed of Cu/ZnO extruded with γ-alumina as a binder. The reaction pressures can be very low as compared to the two-stage process via BDO because the hydrogenation equilibrium between the intermediates GBL and BDO is not limiting when BDO is removed immediately by dehydration over the acidic sites provided by the binder. In addition, it can be anticipated that much less dilution with hydrogen will be required to prevent fouling by polyester deposits in the single-stage gas-phase process. This assumption, however, must still be validated in future experiments.

We have also shown that the forming of Cu/ZnO catalysts by extrusion is an interesting alternative to pelleting. The respective proportions of binder and hydrogenating function can be varied, and the pore texture can be influenced by choice of particle size of the powders used, and by the input of mechanical energy during formulation. It will be a challenging task in the future to analyze quantitatively the interaction among the activities of hydrogenation sites, acid sites, and the diffusional properties of extruded catalysts, and to adjust the balance between these properties for a desired activity and product distribution.

Acknowledgment

We thank Zwick/Roell GmbH for performing the measurements of the bulk crush strengths according to standard ASTM D 4179.

Appendix A. Symbols and abbreviations

c	concentration of Cu- and Zn-carbonate in water-free extrudates; see Eq. (1).
m_i	mass of species i.
p	pressure, Pa.
S_{Cu}	copper surface area, m^2/g.
S_i	reactor selectivity to C_4 product species i; see Eq. (3).
T	temperature, K.
t_{mod}	modified residence time, $g\,s/cm^3$; defined as the ratio of the catalyst mass (basis: total mass of the calcined extrudates loaded into the reactor) to the total volumetric flow at reaction conditions.
WHSV	weight hourly space velocity, h^{-1}; defined as the ratio of the mass flow of dimethyl maleate into the reactor to the catalyst mass (basis: total mass of the calcined extrudates loaded into the reactor).
x_{i,C_4}	molar fraction of C_4 product species i.
X	conversion of dimethyl succinate (conversion of dimethyl maleate is 100%).
GBL	γ-butyrolactone.
BDO	1,4-butanediol.
THF	tetrahydrofuran.

References

[1] H. Müller, in: Industrial Organic Chemicals: Starting Materials and Intermediates (Ullmann's Encyclopedia), Vol. 8, Wiley–VCH, Weinheim, 1999, p. 4621.
[2] ECN, 14 February, 14 (2000).
[3] W. Reppe, E. Keyssner, US patent 2,232,867 (1941).
[4] M.L. Morgan, Chem. Ind. 3 (1997) 166.
[5] K. Weissermel, H.-J. Arpe, Industrial Organic Chemistry, Wiley–VCH, Weinheim, 1997.
[6] M. Sharif, K. Turner, US patent 4,584,419 (1986).
[7] J. Kanetaka, T. Asano, S. Masamune, Ind. Eng. Chem. 62 (1970) 24.
[8] J.H. Schlander, T. Turek, Ind. Eng. Chem. Res. 38 (1999) 1264.

[9] C. Ohlinger, B. Kraushaar-Czarnetzki, Chem. Eng. Sci., in press.
[10] U. Herrmann, G. Emig, Ind. Eng. Chem. Res. 62 (1997) 2885.
[11] U. Herrmann, G. Emig, Chem. Eng. Technol. 21 (1998) 285.
[12] M. Mokhtar, C. Ohlinger, T. Turek, Chem. Eng. Technol. 24 (2001) 423.
[13] M.S. Spencer, in: M.V. Twigg (Ed.), Catalyst Handbook, Wolfe, London, 1989, p. 17.
[14] R.-H. Fischer, F. Stein, R. Pinkos, M. Hesse, M. Sprague, M. Rösch, H. Borchert, S. Schlitter, R.-T. Rahn, A. Weck, German patent application DE 100 61 556 A1, 2002.
[15] H. Borchert, S. Schlitter, M. Rösch, R.-H. Fischer, R.-T. Rahn, A. Weck, German patent application DE 100 61 553 A1, 2002.
[16] G.C. Chinchen, C.M. Hay, H.D. Vanderwell, K.C. Waugh, J. Catal. 103 (1987) 79.